



Regular article

Computational materials design of a corrosion resistant high entropy alloy for harsh environments

Pin Lu^{a,*}, James E. Saal^a, Greg B. Olson^a, Tianshu Li^b, Orion J. Swanson^b, G.S. Frankel^b, Angela Y. Gerard^c, Kathleen F. Quiambao^c, John R. Scully^c

^a QuesTek Innovations LLC, 1820 Ridge Avenue, Evanston, IL 60201, United States

^b Fontana Corrosion Center, The Ohio State University, Columbus, OH 43210, United States

^c Center for Electrochemical Science and Engineering, University of Virginia, Charlottesville, VA 22904, United States

ARTICLE INFO

Article history:

Received 5 April 2018

Accepted 23 April 2018

Available online xxxx

Keywords:

High entropy alloy

Corrosion

CALPHAD

Phase diagram

Modeling

ABSTRACT

The integrated computational materials engineering approach is inherently well suited to explore the vast, multi-dimensional high entropy alloy (HEA) compositional and processing space, and has been adopted in this work, coupled with empiricism, to the design of highly corrosion resistant HEAs. Using the combination of empirical and computational approaches, three non-equi-molar HEA compositions were identified for their predicted ability to form a single-phase structure and to exhibit high corrosion resistance. One of them, $\text{Ni}_{38}\text{Cr}_{21}\text{Fe}_{20}\text{Ru}_{13}\text{Mo}_6\text{W}_2$, was successfully synthesized on the lab-scale and homogenized at 1250 °C for 120 h. Exceedingly high corrosion resistance of the Ni-rich HEA was demonstrated in electrochemical testing.

© 2018 Acta Materialia Inc. Published by Elsevier Ltd. All rights reserved.

Corrosion has become an obstacle to achieving many of the identified engineering grand challenges, according to a recent national academy study [1]. Advancement of technological applications and securing engineering operations in our society demands the design of new corrosion resistant alloys (CRAs) that have superior intrinsic corrosion resistance and are able to resist aggressive corrosion attack in harsh service environments. High entropy alloys (HEAs) are a new class of materials that have exhibited promising characteristics to meet this objective. HEAs comprise single phase solid solutions of five or more elements at or near equimolar composition [2,3]. HEAs are distinct from conventional alloys in that they are not based on one single majority host element, such as Fe in steels, Ni in superalloys, and Al in Al-alloys. Instead, they are composed of multiple principle elements, so they overcome barriers in conventional alloy design and offer vast degrees of freedom in alloy compositions and properties. Numerous studies [4–13] have been conducted to investigate various HEAs with potentially high corrosion resistance. It is worth noting that most of the published studies have focused on HEAs that are equimolar or simple substitutional derivatives of equimolar compositions. However, the corrosion performance of HEAs is not necessarily optimized at such compositions as evidenced by the strong dependence of corrosion resistance on alloy composition and surface oxide film chemistry in compositional complex

alloys and even simple binary alloys [14,15]. Therefore, to identify the most corrosion resistant HEAs, it is important to navigate away from the equimolar trial-and-error approach to corrosion and embark on exploratory routes into the vast, non-equi-molar compositional space.

The scarcity of corrosion studies on complex non-equi-molar HEAs is partly due to the limitations of the conventional empirical approach to CRA design, which is usually costly, incremental and time-consuming. Such drawbacks become more prominent when it comes to designing and synthesizing HEAs, where the myriad possibilities in the multi-dimensional compositional space are too large to tackle by experimental approaches alone. There is clearly a need for an advanced approach to design CRAs and especially corrosion resistant HEAs (CR-HEAs). Integrated computational materials engineering (ICME) is a modern systems-based approach to design materials that meet specific performance criteria by linking computational materials models across multiple length scales [16]. The ICME approach can readily predict many properties for an alloy based on tools such as Calculation of Phase Diagrams (CALPHAD) and Density Functional Theory (DFT), provided accurate databases of materials behavior are available. Thus, ICME is ideally suited to efficiently and exhaustively search for and design CR-HEAs with sought-after attributes. Mechanistic corrosion models for predicting corrosion resistance quantitatively from alloy composition on a fundamental scientific level are currently being actively developed [17], but are not yet mature enough to be incorporated into an ICME framework. However, it is possible to combine empirical corrosion resistance paradigms based on prior knowledge with computational tools to identify promising CR-HEAs [17].

* Corresponding author.

E-mail address: plu@questek.com (P. Lu).

In this paper, we report a design process using a combination of empiricism and computation that has led to successful identification of several single-phase non-equimolar CR-HEAs showing great potential for superior corrosion resistance. The present study has mainly focused on single-phase HEAs, as the development of homogeneous solid solution alloys with minimization of structural and chemical heterogeneities is the most typical strategy for CRA design with the greatest chance for superior corrosion resistance. One of the designed CR-HEAs has been successfully synthesized and has experimentally demonstrated single phase stability and exceedingly high corrosion resistance, even in very harsh testing environments.

The pitting resistance equivalent number (PREN) [18,19], a linearized fit of the wt% of certain constituent alloy elements to corrosion performance parameters, initially derived for Fe-based CRAs has been considered. Various equations for PREN have been developed from numerical fitting of elemental concentrations in Fe-Cr-Ni alloys to experimentally determined corrosion parameters, such as critical pitting potential and critical pitting temperature [20,21]. PREN is a simple correlation that is useful for predicting corrosion resistance of Fe-based stainless steels. The approach has been extended to Ni base super alloys [22–25] and iron-based metallic glasses [26]. In both cases, a qualitative trend was found, but the database is not extensive enough to establish a strong relationship for wide-ranging compositions. Moreover, PREN lacks a scientific basis for capturing the underlying mechanism that governs the effects of those beneficial alloying elements, making it difficult to apply PREN to alloys that include elements other than those found in Fe-based CRAs (such as those elements found in HEAs). PREN also lacks consideration of microstructure, environment or interactions between alloying elements.

The PREN approach has been used in this work, but discretion has been exercised and additional ICME tools and guidance have been employed complementarily in an attempt to extrapolate PREN beyond the fitted data and into new HEA compositional space. It is possible to design an alloy that has sufficiently high configurational entropy to be considered an HEA, but remains chemically akin to Fe-based stainless steels and Ni-based superalloys (e.g., enriched in Fe or Ni), such that the PREN approach may still be used for semi-quantitative prediction of corrosion resistance. The PREN used in the present work is defined as $\text{PREN} = \text{wt. \% Cr} + 3.3 (\text{wt. \% Mo} + 0.5 \text{ wt. \% W})$, a version taking in account the positive influence of W in addition to Cr and Mo on pitting resistance [25,27,28].

Backed by this rationale, two initial HEA compositions, one enriched in Fe and the other enriched in Ni as specified in Table 1, have been conceived based on prior corrosion and metallurgical paradigms: 1) Cr, Mo, W can effectively improve corrosion resistance according to the PREN model; and 2) Ru is useful to effectively suppress topologically closed packed phases and promote single phase formation [29]. These two compositions represent the HEA compositional spaces where the aforementioned corrosion-enhancing elements are combined. Thermo-Calc with the TCHEA2 database [30] was utilized to identify specific HEA compositions that have a wide temperature window over which a single phase is stable with the goal of quenching to a single phase structure at ambient temperature and enabling proper homogenization. This database has been demonstrated to have excellent agreement with the experimental HEA phase stability studies [31].

Table 1
HEAs designed based on prior corrosion paradigm and predicted single phase by CALPHAD in Thermo-Calc software with TCHEA2 database.

| Initial compositions (at.%) | Stable phases (at.%) | Structure | ΔS_{conf} | PREN |
|--|--|-----------|--------------------------|------|
| Fe ₃₀ Cr ₂₀ Mn ₂₀ Ru ₂₀ Mo ₅ W ₅ | Fe ₃₀ Cr ₂₅ Mn ₂₅ Ru ₁₀ Mo ₆ W ₄ | BCC | 1.58R | 64 |
| | Fe ₃₂ Ru ₃₀ Cr ₁₄ Mn ₁₄ W ₆ Mo ₄ | HCP | 1.59R | 50 |
| Ni ₃₀ Cr ₂₀ Fe ₂₀ Ru ₂₀ Mo ₅ W ₅ | Ni ₃₈ Cr ₂₁ Fe ₂₀ Ru ₁₃ Mo ₆ W ₂ | FCC | 1.53R | 54 |
| | Ru ₄₂ Fe ₂₁ Cr ₁₅ W ₆ Ni ₄ Mo ₁ | – | – | – |

The thermodynamic properties of the two initial compositions were calculated at 1100 °C, a high temperature assumed high enough to solutionize the HEAs into a single phase. The results indicate that both compositions are unstable at 1100 °C and each will decompose into two stable phases (Table 1). Among the four new phases, one is rich in Ru (Ru₄₂Fe₂₁Cr₁₅W₆Ni₄Mo₁) and was therefore excluded from further consideration. The other three are disordered solid solutions of BCC and FCC, enriched either in Fe or Ni, mimicking to some extent the chemistry of stainless steels and superalloys for which PREN has been successfully applied. The predicted structure, configurational entropy, and PREN of those three phases are presented in Table 1. Their ΔS_{config} are all >1.5R, a conventional threshold value above which an alloy can be deemed to be an HEA [32], and their PRENs are comparable to those of commercial super stainless steels and nickel-based superalloys. The results above suggest that the three compositions predicted to be stable at 1100 °C all can form single-phase HEAs that potentially possess superior corrosion resistance as reflected by their high PRENs. In particular, the Ni-rich FCC-based HEA, Ni₃₈Cr₂₁Fe₂₀Ru₁₃Mo₆W₂, was selected for further CALPHAD evaluations and experimental validation in this study. To assess the ability of this HEA to form a single phase, a pseudo-binary phase diagram was created, as shown in Fig. 1, where Cr content is varied and balanced by Ni. This diagram shows the amount of Cr that can be substituted by Ni at different temperatures while still retaining the single FCC phase, which aids in exploration of non-equimolar HEAs in a single-phase structure. It can be observed that this particular HEA composition space has a fairly broad single phase region in terms of tolerance in Cr variation, along with wide temperature windows (span of 300 °C–400 °C) at various Cr levels, which are indications of ease of solutionizing and good processability. This phase diagram is also useful for identifying a stable composition range over which systematic changes in elemental concentration could be explored (e.g., to study the effects of different elements on corrosion).

To explore the thermodynamic stability of the oxide film formed on the HEA in water of various pH levels under oxidizing and reducing conditions, stability regions of oxides in the electrochemical potential/pH domain for Ni₃₈Cr₂₁Fe₂₀Ru₁₃Mo₆W₂ were computed by a modified version of CALPHAD in Thermo-Calc software (Fig. 2). The calculation conditions were 25 °C, 1 atm, 1 kg of H₂O with 0.6 M NaCl, and the total alloy amount was 10^{−2} mol. The databases employed were TCAQ3, AQS2, SSUB3, and TCHEA2 [30]. TCAQ3 plus AQS2 contain most of the aqueous species for the composing elements, except Mo³⁺. Due to this absence, the stability region of Mo³⁺ was manually incorporated by superimposing the E-pH diagram for pure Mo, which contains an Mo³⁺ region [33], onto the calculated diagram. SSUB3 includes all the six

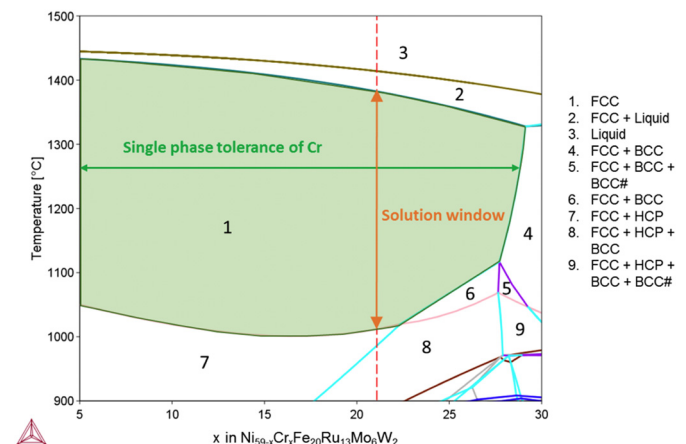


Fig. 1. Pseudo-binary phase diagram of Ni_{59-x}Cr_xFe₂₀Ru₁₃Mo₆W₂ calculated in Thermo-Calc with TCHEA2 database. The FCC single phase region is shaded in green. The dashed line corresponds to the Ni-rich HEA composition with 21 at.% Cr. BCC and BCC# are two disordered BCC phases with a miscibility gap. (For interpretation of the references to colour in this figure legend, the reader is referred to the web version of this article.)

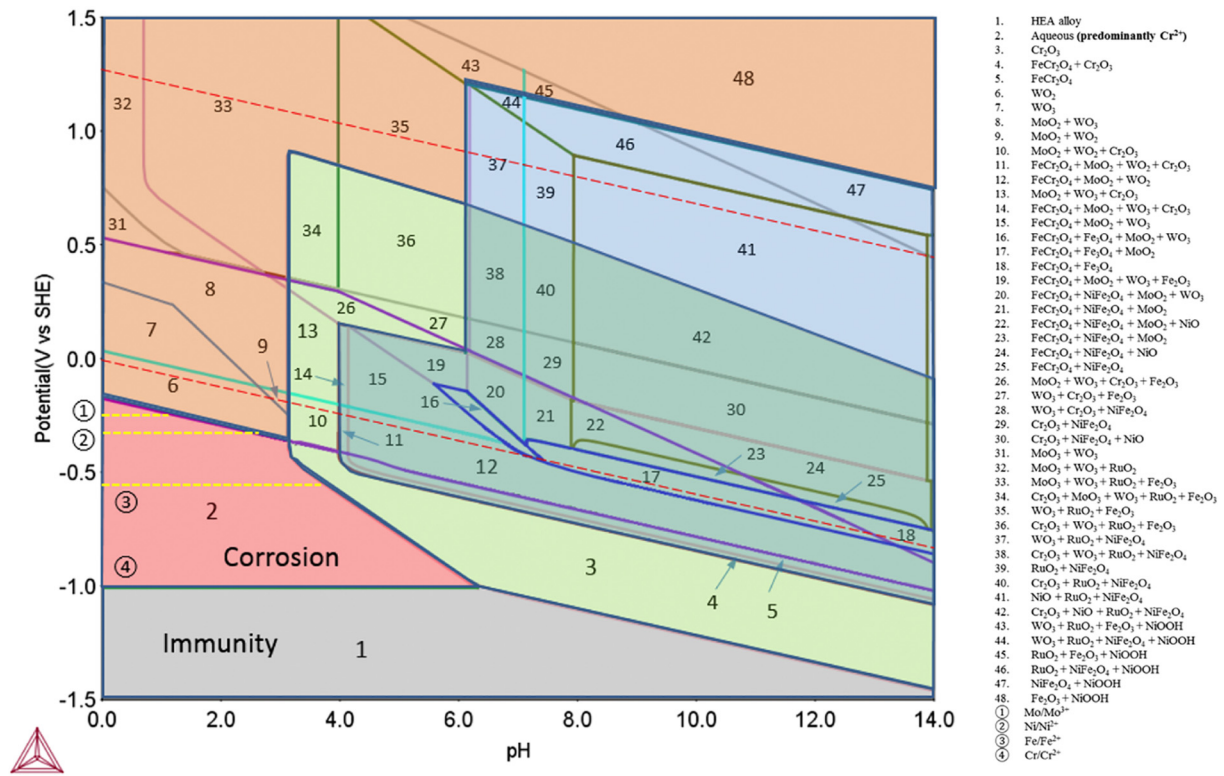


Fig. 2. CALPHAD-calculated E - pH diagram for $Ni_{38}Cr_{27}Fe_{20}Ru_{13}Mo_6W_2$ in 1 kg H_2O at 25 °C and 1 atm. The amounts of metal solutes were $N(Ni) = 38 \times 10^{-4}$ mol, $N(Cr) = 21 \times 10^{-4}$ mol, $N(Fe) = 20 \times 10^{-4}$ mol, $N(Ru) = 13 \times 10^{-4}$ mol, $N(Mo) = 6 \times 10^{-4}$ mol, $N(W) = 2 \times 10^{-4}$ mol. The red dashed lines are reversible potentials for hydrogen and oxygen evolutions, and the yellow dashed lines are the metal/aqueous ion equilibrium lines for pure constituent elements. Red region indicates where oxidized aqueous species are stable, green region indicates where Cr_2O_3 is stable, blue region indicates where Fe-Ni, Fe-Cr spinels are stable with part overlapping with the green region, and orange region indicates where other oxides are stable. (For interpretation of the references to colour in this figure legend, the reader is referred to the web version of this article.)

elements as single oxides/hydroxides, spinels, and molybdates and tungstates. The FCC phase in TCHEA2 was included to describe the FCC HEA matrix. As described previously [19], gas phases and components in the databases were excluded from the calculations to reveal the complete stability regions of non-gaseous phases (i.e. aqueous, metal, oxides), which otherwise will be covered over by gas phase regions. A corrosion-immune region can be seen at low potentials and an aqueous corrosion region where aqueous species are thermodynamically stable exists at low pH values. Note that this aqueous region indicates where at least one (and not necessarily all) of the constituent elements forms a stable oxidized aqueous phase. For clarification, the metal/aqueous ion equilibrium lines for constituent elements were calculated separately in Thermo-Calc and shown the diagram (dotted yellow lines and labeled by circled numbers in Fig. 2). Protective oxides (e.g., Cr_2O_3 , Cr-containing spinels) are predicted to form throughout the remainder of the E - pH space. Note that, as is the case for all E - pH diagrams, thermodynamically stable oxides do not ensure passivation will occur in an actual environment.

For experimental validation of the designed HEA, button samples were prepared by arc-melting using pure elemental metals (>99.9% trace metals basis) under a purified argon gas atmosphere. To obtain a completely alloyed state, the buttons were flipped and re-melted multiple times with at least 30 min in the liquid state. The as-cast button was then encapsulated in quartz filled with argon gas and homogenized at 1250 °C (based on Fig. 1) for 120 h. The button was then water-quenched to ensure a homogenous single-phase structure, which was confirmed by scanning electron microscopy/energy-dispersive X-ray spectroscopy and x-ray diffraction. The corrosion resistance of the HEA button was evaluated by polarization and electrochemical impedance spectra (EIS) testing in two environments: air-exposed 6 M HCl and deaerated 0.1 M $Na_2SO_4 + H_2SO_4$ (pH = 4), both at ambient temperature. Polycrystalline alloy C-22 (59Ni-22Cr-3Fe-16Mo-3 W; wt%)

was also tested in the sulfate solution for comparison. A three-electrode cell was used with a platinum mesh as the counter electrode, and a saturated calomel electrode (SCE) or mercury-mercurous sulfate electrode (MMSE) as reference electrode in the chloride or sulfate electrolyte, respectively. For polarization in 6 M HCl, the open circuit potential (OCP) was monitored for 10 min and then the potential was scanned upwards at 0.33 mV/s from -200 mV vs. OCP and reversed at a current density of 10^{-3} A/cm² with a scan rate of 1 mV/s. Anodic polarization in the sulfate solution was performed by scanning the potential from -1.71 V_{MMSE} to 0.39 V_{MMSE} at 0.5 mV/s. Potentiostatic EIS measurements at the OCPs after 24 h of OCP exposure were conducted on the HEA over frequencies from 100 kHz to 1 mHz with a sinusoidal potential of 20 mV_{rms}. The polarization results are shown in Fig. 3.

The OCP of the HEA upon immersion in 6 M HCl was found to drift upwards with time, suggesting spontaneous passivity, which was confirmed by the polarization curve. The pH of 6 M HCl is below zero. Since no stable equilibrium oxides are predicted for this region of the E - pH diagram, the experimental observation of passivity implies the presence a metastable oxide that forms and grows faster than it dissolves in this solution. The passive current density in Fig. 3(a), on the order of 10^{-5} A/cm², varied only slightly with increasing potential over a wide range. The current increased markedly at potentials above about 700 mV_{SCE}. The negative hysteresis observed upon scan reversal indicates that this increase was caused by transpassivity rather than localized corrosion, which was confirmed by the lack of pits or crevices on the sample after testing. Furthermore, no current transients that might be associated with metastable pitting were observed. It has been suggested that 5 M HCl can be used to simulate the aggressive environment inside a real pit in a CRA [34]. Thus the 6 M HCl bulk test solution would be more aggressive than the pitting environment that could spontaneously generate if pitting did occur. The strong and spontaneous passivity persisting to high potentials in such an extremely aggressive

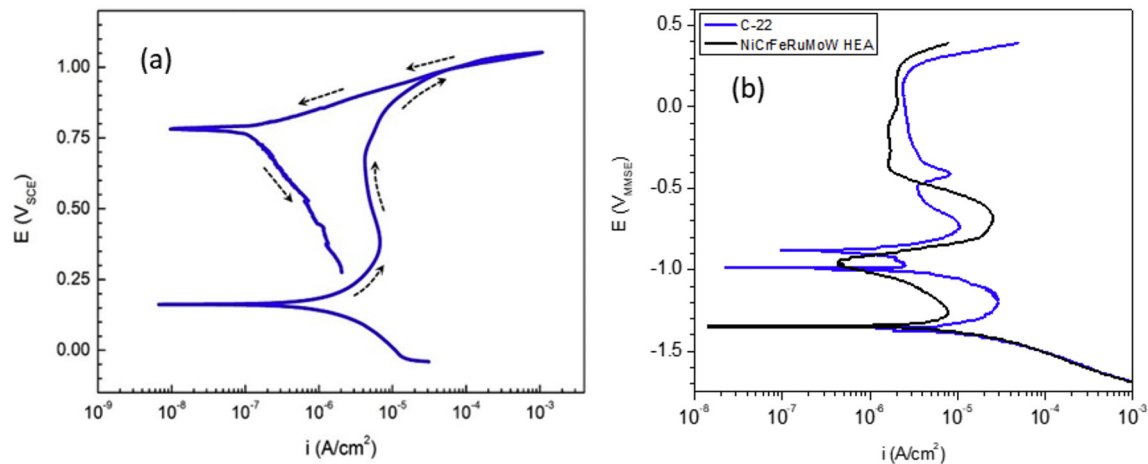


Fig. 3. Polarization curves of $\text{Ni}_{38}\text{Cr}_{21}\text{Fe}_{20}\text{Ru}_{13}\text{Mo}_6\text{W}_2$ HEA at ambient temperature in (a) 6 M HCl solution exposed to air, and (b) deaerated 0.1 M $\text{Na}_2\text{SO}_4 + \text{H}_2\text{SO}_4$ (pH = 4).

environment indicates this HEA possesses extremely high resistance to pitting corrosion, and can even be considered to be immune to pitting. The polarization results of HEA and C-22 in the sulfate solution are compared in Fig. 3(b), where the HEA exhibits a passive region as wide as C-22 but with lower passive current densities at most potentials, demonstrating the exceedingly high corrosion resistance of the HEA, despite the fact that the HEA has a smaller PREN than C-22 (54 vs. 70). This clearly demonstrates the limitation of using PREN as a quantitative indicator of corrosion resistance for CR-HEA design. EIS results (not shown here) indicated a single time constant with capacitive behavior over a wide range of frequency and low frequency impedance approximately $10^6 \Omega\text{-cm}^2$ that changed little with time. Polarization resistance (R_p) after 24 h OCP exposure were determined from the EIS results: $6.37 \times 10^5 \Omega\text{-cm}^2$ and $3.00 \times 10^6 \Omega\text{-cm}^2$ in 6 M HCl and the sulfate solution, respectively. Utilizing the Stern-Geary equation [35,36], $R_p = \beta_a\beta_c / 2.3i_{\text{corr}}(\beta_a + \beta_c)$, where β_a and β_c are Tafel slopes for the anodic and cathodic reactions, respectively, corrosion current density, i_{corr} , may be calculated. For example, by assuming β_a to be infinite within the passive region and β_c to be 120 mV/dec, i_{corr} in the sulfate solution after 24 h OCP hold can be calculated to be $1.74 \times 10^{-8} \text{ A/cm}^2$, which is extremely small.

In summary, it is shown that CALPHAD computational tools combined with empirical knowledge can guide the selection of corrosion resistant, single-phase HEA compositions, one of which was demonstrated to indeed possess exceedingly high corrosion resistance, even in very harsh environments. The successful validation of the computational design efforts with pre-set property goals shows that ICME is suitable for corrosion resistant HEA design, including complex non-equimolar HEAs.

Acknowledgements

This work was supported as part of the Center for Performance and Design of Nuclear Waste Forms and Containers, an Energy Frontier Research Center funded by the U.S. Department of Energy, Office of Science, Basic Energy Sciences under Award # DE-SC0016584. Dr. Dan Schreiber is gratefully acknowledged for reviewing the paper and providing numerous helpful suggestions.

References

- [1] NAE Grand Challenges for Engineering, National Academy Press, 2008.
- [2] J.W. Yeh, S.K. Chen, S.J. Lin, J.Y. Gan, T.S. Chin, T.T. Shun, C.H. Tsau, S.Y. Chang, *Adv. Eng. Mater.* 6 (2004) 299.
- [3] M.H. Tsai, J.W. Yeh, *Mater. Res. Lett.* 2 (2014) 107.
- [4] C.P. Lee, C.C. Chang, Y.Y. Chen, J.W. Yeh, H.C. Shih, *Corros. Sci.* 50 (2008) 2053.
- [5] Y.L. Chou, J.W. Yeh, H.C. Shih, *Corros. Sci.* 52 (2010) 2571.
- [6] B. Ren, Z.X. Liu, D.M. Li, L. Shi, B. Cai, M.X. Wang, *Mater. Corros.* 63 (2012) 828.
- [7] X.W. Qiu, Y.P. Zhang, L. He, C.G. Liu, *J. Alloys Compd.* 549 (2013) 195.
- [8] Y. Qiu, M. Gibson, H. Fraser, N. Birbilis, *Mater. Sci. Technol. Lond.* 31 (2015) 1235.
- [9] V. Soare, D. Mitrica, I. Constantin, G. Popescu, I. Csaki, M. Tarcolea, I. Carcea, *Metall. Mater. Trans. A* 46A (2015) 1468.
- [10] Z. Zhang, E. Axinte, W. Ge, C. Shang, Y. Wang, *Mater. Des.* 108 (2016) 106.
- [11] D.B. Miracle, O.N. Senkov, *Acta Mater.* 122 (2017) 448.
- [12] Y. Qiu, S. Thomas, M.A. Gibson, H.L. Fraser, N. Birbilis, *npj Mater. Deg.* 1 (2017) 15.
- [13] Y. Qiu, S. Thomas, M. Gibson, H. Fraser, K. Pohl, N. Birbilis, *Corros. Sci.* 133 (2018) 386.
- [14] C. Lee, Y. Chen, C. Hsu, J. Yeh, H. Shih, *Thin Solid Films* 517 (2008) 1301.
- [15] Q. Li, T. Yue, Z. Guo, X. Lin, *Metall. Mater. Trans. A* 44 (2013) 1767.
- [16] C. Kuehmann, G. Olson, *Mater. Sci. Technol. Lond.* 25 (2009) 472.
- [17] C.D. Taylor, P. Lu, J. Saal, G. Frankel, J. Scully, *npj Mater. Deg.* 2 (2018) 6.
- [18] N. Dowling, Y.H. Kim, S.K. Ahn, Y.D. Lee, *Corrosion* 55 (1999) 187.
- [19] G. Herbsleb, *Mater. Corros.* 33 (1982) 334.
- [20] K. Lorenz, G. Medawar, *Thyssenforschung* 1 (1969) 97.
- [21] R. Jargelius-Pettersson, *Corrosion* 54 (1998) 162.
- [22] F. Wong, The Effect of Alloy Composition on the Localized Corrosion Behavior of Ni-Cr-Mo Alloys Ph.D. thesis The Ohio State University, 2009.
- [23] F. Bocher, R. Huang, J. Scully, *Corrosion* 66 (2010), 055002.
- [24] N. Zadorozne, C. Giordano, M. Rodríguez, R. Carranza, R. Rebak, *Electrochim. Acta* 76 (2012) 94.
- [25] R.M. Carranza, M.A. Rodríguez, *npj Mater. Deg.* 1 (2017) 9.
- [26] R. Huang, D. Horton, F. Bocher, J. Scully, *Corrosion* 66 (2010), 035003.
- [27] S.S. Haudet, M.A. Rodríguez, R.M. Carranza, R.B. Rebak, *Corrosion* 2012, NACE International, 2012.
- [28] A. Mishra, D. Shoesmith, *Corrosion* 70 (2014) 721.
- [29] A. Sato, H. Harada, T. Yokokawa, T. Murakumo, Y. Koizumi, T. Kobayashi, H. Imai, *Scr. Mater.* 54 (2006) 1679.
- [30] <http://www.thermocalc.com/products-services/databases/thermodynamic/>.
- [31] J.E. Saal, I.S. Berglund, J.T. Sebastian, P.K. Liaw, G.B. Olson, *Scr. Mater.* 146 (2018) 5.
- [32] M.C. Gao, J.W. Yeh, P.K. Liaw, Y. Zhang, *High-Entropy Alloys: Fundamentals and Applications*, Springer International Publishing, 2016.
- [33] T. Kodama, J. Ambrose, *Corrosion* 33 (1977) 155.
- [34] V.M. Salinas-Bravo, R.C. Newman, *Corros. Sci.* 36 (1994) 67.
- [35] D.A. Jones, *Principles and Prevention of Corrosion*, second ed. Prentice-Hall, Inc., Upper Saddle River, 1996.
- [36] E. McCafferty, *Introduction to Corrosion Science*, Springer, New York, 2010.